Comprehensive Journal of Science
Volume (10), Issue (37), (NOV. 2025)
SICST2025, www.sicst.ly
ISSN: 3014-6266

مجلة العلوم الشاملة
عدد خاص بالمؤتمر الدولي الثالث للعلوم والتقنية
المجلد (10)، العدد (37)، (نوفمبر2025)
ردمد: 3014-6266

Design of a Permanent-Magnet Fault Current Limiter for Low-Voltage Industrial Applications.

Asmaiel Ramadan[1], Aimen Matoug[2], Khaled Elshibani[3]

Department of Electrical Engineering

The Higher Institute of Science and Technology, Tarhuna, Libya

asmailramadan@gmail.com aimenmatoug11@yahoo.com K.alshebane@yahoo.com

تصميم مُحدِّد تيار عطل بالمغناطيس الدائم للتطبيقات الصناعية ذات الجهد المنخفض

إسماعيل رمضان[1]، أيمن معتوق[2]، خالد الشيباني[3]

قسم الهندسة الكهربائية، المعهد العالي للعلوم والهندسة، ترهونة – ليبيا

Received: 30-09-2025; Revised: 10-10-2025; Accepted: 31-10-2025; Published: 25-11-2025

Abstract

The permanent magnet fault current limiter (PMFCL) offers several significant advantages, including compactness, high reliability, zero reset time, safe operation, and inherent fail-safe characteristics, making it a highly viable solution for moderating fault currents in power system networks. This paper presents the design of a low-voltage (480 V) PMFCL. The proposed industrial device can be used with the existing oil production 480V motor control center (MCC) switchgear facilities across Libya and considerably for other proposed future renewable energy sources.

Three-dimensional finite element method (3D FEM) simulations confirm that the advanced industrial low voltage PMFCL device operates effectively and reliably under both fault conditions and normal operation within the power distribution network.

Keywords— *Fault current limiter*; FEM; air-cored; Low voltage; switchgear

ملخـــص البحـــث

المحدد الدائم لمحدود تيار القصر (**PMFCL**) يقدم عدة مزايا مهمة، منها الحجم المدمج، والموثوقية العالية، وانعدام زمن إعادة الضبط، والتشغيل الآمن، وخصائص الأمان الذاتي الفطرية، مما يجعله حلاً فعالاً للغاية للحد من تيارات القصر في شبكات أنظمة الطاقة. تعرض هذه الورقة تصميم محدد تيار قصر منخفض الجهد (480 فولت) من نوع **PMFCL**. يمكن استخدام هذا الجهاز الصناعي المقترح مع مرافق لوحات التحكم في المحركات (**MCC**) بجهد 480 فولت الموجودة في حقول إنتاج النفط في ليبيا، وكذلك بشكل كبير مع مصادر الطاقة المتجددة المقترحة مستقبلاً.. تؤكد عمليات المحاكاة باستخدام طريقة العناصر المحدودة ثلاثية الأبعاد (**3D FEM**) أن جهاز المحدد الدائم لمحدود تيار القصر **PMFCL** الصناعي المتطور منخفض الجهد يعمل بكفاءة وموثوقية سواء في ظروف الأعطال أو أثناء التشغيل الطبيعي ضمن شبكة توزيع الطاقة الكهربائية.

الكلمات الدالة: مُحدِّد تيار العطل; طريقة العناصر المحدودة; قلب هوائي; جهد منخفض; معدات التوزيع الكهربائي.

Introduction

Fault currents are generally momentary disturbances initiated by various factors such as equipment malfunctions, lightning strikes, vegetation encroachment, or, in some cases, animals causing short circuits within the power distribution network. In all cases, the resulting transient current surges can easily damage transmission lines, power generation units, and substation components. Under certain conditions, faults can propagate through the network, potentially affecting large sections of the power grid and leading to widespread blackouts that extend across multiple countries or states. [1]. A significant concern in power system operation is the voltage depression that occurs during fault conditions. Voltage dip or voltage sag due to a fault on a power distribution transformer can affect the power system equipment such as the generator unit out of step and is the most crucial power quality concern [2],[3]. The reduction of the fault current is a long-standing issue for power systems engineering. Fault current reduction facilitates the integration of extensive power networks without requiring infrastructure replacement, does not cause the system to lose its stability after the fault occurrence, and reduces equipment costs. With the ongoing advancements in magnetic materials and topology optimization, fault current limiters utilizing permanent magnet biased saturation have recently attracted considerable attention from the scientific and research communities. A Fault Current Limiter (FCL) is a variable impedance device connected in series with a circuit breaker. It has a negligible impact on the power system under normal operating conditions; however, it becomes active during transient events by limiting the fault current [4]-11]. The work presented in this paper was performed on a 480V ring shaped topology model. The design was specifically developed to meet the electrical power supply requirements of existing oil production facilities in Libya. In oil production facilities across Libya, the 480 V low-voltage electrical system is widely adopted for a variety of industrial applications. This voltage level is typically used to supply power to three-phase induction motors, auxiliary systems, control units, and general lighting infrastructure [12]. However, this specific industrial low voltage device can be used for the future solar power unit in Libya oil fields and considerably for other renewable energy sources [13], [14]. The 3D Finite Element Method (FEM) simulation tool, MagNet, was employed in the design of the PMFCL device. MagNet applies Maxwell's equations to simulate and analyse electromagnetic problems on personal computers. [15]. In this work, the initial design of the PMFCL device was obtained using derived equations to determine the appropriate dimensions of the model. The required flux density provided by the Neodymium–Iron–Boron (NdFeB) to achieve core saturation was calculated systematically. Once the initial dimensions were established, the model was developed using the finite element method (FEM). The flux density was then evaluated through FEM simulations, with several iterations performed to ensure the desired extent of

core saturation. This comparative analysis confirmed the accuracy of the simulation model and its ability to replicate the physical magnetic behavior within the core. Following validation, the steady-state characteristics of the current against inductance was simulated and plotted in three dimensions to investigate the change of inductance with the increased load current. This analysis yielded valuable insights into the device's magnetic saturation behavior and its influence on inductive reactance under both steady and abnormal conditions. Finally, the transient response of the PMFCL was examined through time-dependent 3D modelling. This process involved simulating dynamic electromagnetic behavior during fault events to assess the device's effectiveness in limiting fault currents while maintaining stability after the fault event. The transient analysis further enabled the evaluation of potential thermal and mechanical stresses induced by rapid current fluctuations.

PMFCL PRINCIPLE OF OPERATION

The ring-shaped PMFCL structure is depicted in Figure 1, which presents a three-dimensional schematic of the proposed design. The configuration consists of two neodymium magnets, grain oriented electrical steel core M16, and three pairs of copper coils wound around the core. The neodymium magnet was selected because of its exceptionally high magnetic strength, coercivity and maximum energy product [16]. The magnetic flux path to the M16 core is through low carbon steel intermediate-pole. The intermediate pole supports the magnets in position and controls the transfer of the uniform magnetic flux to provide the necessary magnetic excitation for the M16 grain oriented electrical steel core. Furthermore, the presence of the steel pole eliminates the air gap between the magnets, thereby reducing the flux leakage. In addition, the model ring shaped symmetrical design confirms that only a negligible amount of magnetic flux escapes the core, as a result the excitation efficiency of the core is maximized. The state-of-the-art device incorporates three pairs of short length copper coils (six coils in total), each consisting of 8 turns wound uniformly around the ring-shaped core. The coils are wounded from enamel-insulated copper wire selected to a suitable gauge to carry the expected operating current while minimizing resistive losses. As the core has no corners, the flux flows efficiently in the closed ring path. This in turn leads to improved magnetic characteristics and enhanced performance capabilities over other topologies. The ring core topology with increased inner radius and reduced radial thickness offers high efficiency with reduced operating losses and overall cost. Furthermore, it is lighter, more compact, and easier to install. [17].

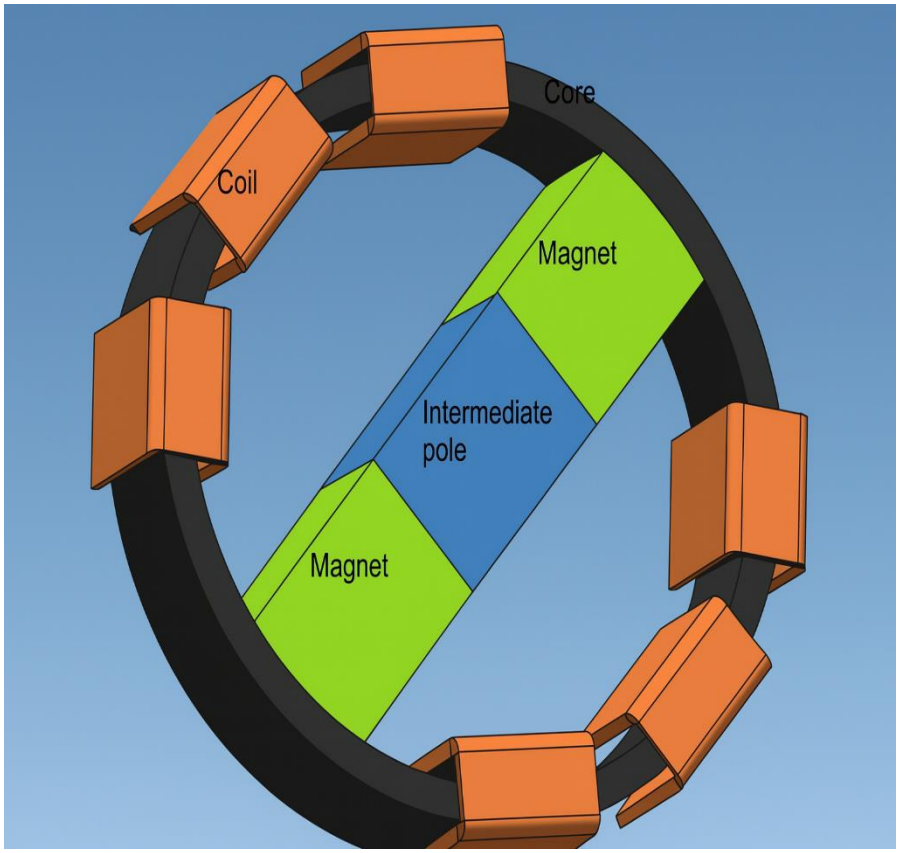

Figure 1 schematic diagram of the ring topology

The general expression for the flux density in a series magnetic circuit is given by:

$$2(H_c l_m - \phi_m R_m) - \phi_{ip} R_{ip} - \phi_c R_c + 6\,ni = 0 \qquad (1)$$

Where (m), (ip) and c refer to the magnet, steel inter-pole and the M16 core. The nneodymium magnet Coercivity $H_c = 8.68 \times 10^5 \frac{A}{m}$ and R is the magnetic circuit reluctance. The magnets and AC coils are configured with the same polarity so that, during each half cycle of the alternating current, three coils on one side of the core ring oppose the magnetic field generated by the magnets. Consequently, the flux density in the core can be calculated as

$$2(H_c l_m - \phi_m R_m) - \phi_{ip} R_{ip} - \frac{\phi_c}{2} R_c + 3\,ni = 0 \qquad (2)$$

$$2(H_c l_m - \phi_m R_m) = \phi_{ip}\, R_{ip} + \frac{\phi_c}{2} R_c + 3\,ni \qquad (3)$$

The magnetic field in each section of the core is the same, (ϕ_c), (ϕ_m) and (ϕ_{ip}) are the same. The magnetic flux density in the core can be obtained from equation 4.

$$\phi_c = \frac{H_c\ l_m + 1.5\,ni}{R_m + \ 0.5\ R_{ip} + 0.25\,R_c} \qquad (4)$$

The initial design justifies a full magnetic saturation of the core, which is then confirmed by the Magnet 3D FEM simulation tool.

Table 1, PMFCL model parameters

Component /parameters	Material	Dimensions (m) / turns	Cross section (m^2)
Magnet	Neodymium (NdFeB)	0.28 x 0.21 x 0.34	0.28 x 0.21= 0.0596
Ring core	M16 steel	Internal radius = 0.42 external radius = 0.46	0.11
Intermediate pole	Steel 1010	0.28 x 0.21 x 0.34	0.28 x 0.21 = 0.0596
Coil (each)	Copper	0.25 x 0.045 x 0.01	0.25 x 0.045 = 0.011
Phase voltage (volt)	----------	480 / 1.731	----------
Normal current	----------	1015 A	----------
Frequency	----------	60 Hz	----------

THE MODELLING RESULTS.

Once the model's initial specifications were systematically established, the design tool was used to simulate the device by assigning appropriate materials to each component — including the magnet, core, intermediate pole, and coils. Mesh refinement was applied with particular attention to the core and coil zones to ensure reliable and fruitful results. The FEM model was then assessed for core saturation under zero AC excitation conditions. This step was carried out to verify the biasing capability of the magnet, ensuring that the device can maintain precise performance and high efficiency under both normal and dynamic operating conditions. The standard magnetostatic solver was employed to visualise the core's magnetic flux density and identify any regions approaching saturation when no AC excitation was applied.

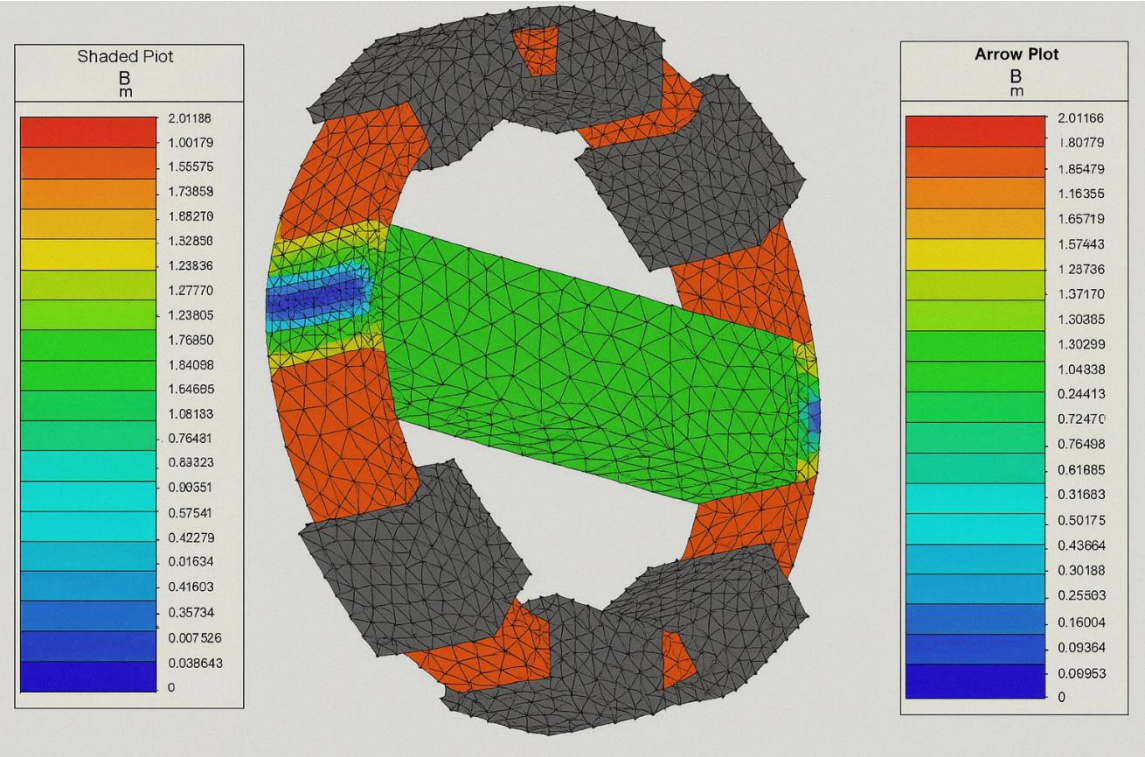

Figure 2: M16 Flux density distribution

The magnet must have a strong capability to provide the core with the required saturation extent. The core is considered to reach the saturation level when the flux density is about two Tesla. The finite element analysis (FEA) simulation result shows that the magnetic flux density is uniformly distributed within the conductor region, while the core reaches adequate magnetic saturation. The figure shows the Left side (Shaded Plot) and the arrow plot on the right. The high flux density is indicated by red regions where the core is in full saturation up to 2.1 Tesla. The flux density ranges from a low value with blue regions and gradually to the highest value where the coils are close to the magnets. This means that the neodymium magnets are successfully driving enough flux into the M16 steel via the low-carbon steel intermediate-pole to achieve a strong working flux in the coil region

The next essential design step is the inductance against current graph. Figure 3 shows Inductance (μH) on the Y-axis against RMS current (kA) on the x-axis. Inductance starts around 120 μH at very low current. It rises sharply to a peak around 320 μH. After the peak, inductance gradually decreases, dropping back near 120 μH by around 7.2 kA. This kind of behaviour suggests nonlinear magnetic properties, likely due to core saturation effects. The maximum inductance value determines the PMFCL short circuit capacity. As illustrated in the figure an inductance of 320μH at a coincident current level of 2300A_{rms}. Therefore, the device rated fault withstand current is predicted to be almost equal

to the peak value of the maximum calculated RMS current, approximately 3220 A.

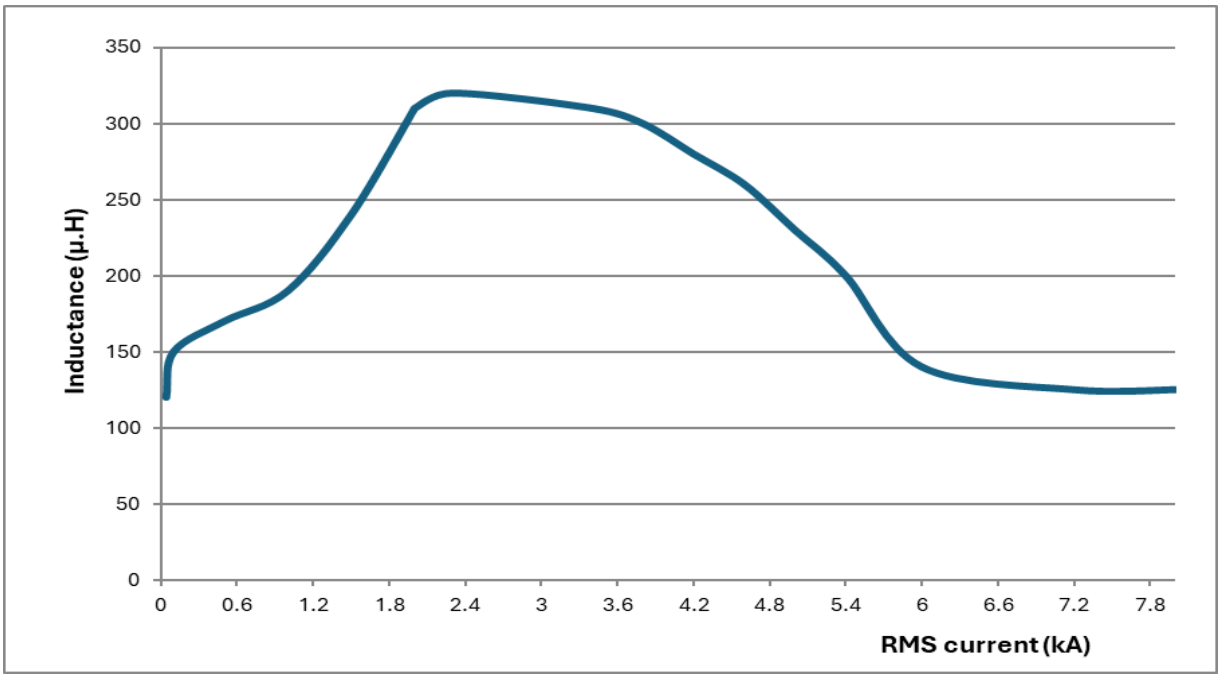

Figure 3 inductance against current graph

The analysis was conducted using a three-dimensional finite element transient problem solver to analyse the fault current operation. The electrical circuit shown in figure 4 is associated with the finite element magnetics (FEM) model. The circuit is supplied by the peak phase voltage source $V1$ and drives current through the six series connected coils that are linked magnetically to the PMFCL coils.

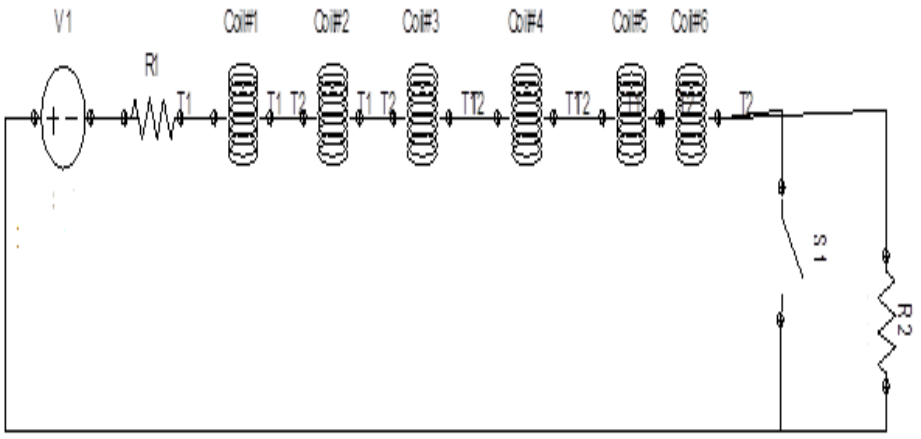

Figure 4 Transient circuit simulation

The circuit exhibits an input resistance of 0.018 Ω, in addition to a stray resistance of 0.15 Ω. The peak amplitude of the single-phase voltage source applied to one half of the model is 195V. Coupling between the power circuit and the PMFCL finite element model (FEM) is established through shared nodes. Initially, the circuit runs under normal operating conditions for two electrical cycles with the switch $S1$ open, allowing current to flow through the load resistor $R2$. After two cycles, the switch $S1$ is closed to simulate a fault condition by creating a low-impedance path. This sudden change in circuit impedance results in a rapid increase in current, which is used to study the PMFCL's transient response and its resulting fault current limiting performance. The normal current of 1015 A was calculated over a two-cycle period preceding the fault occurrence. The fault event is triggered when switch S1 closes, causing a sudden change in the circuit conditions. The performance data for the PMFCL is compared against that of an equivalently sized air-cored device.

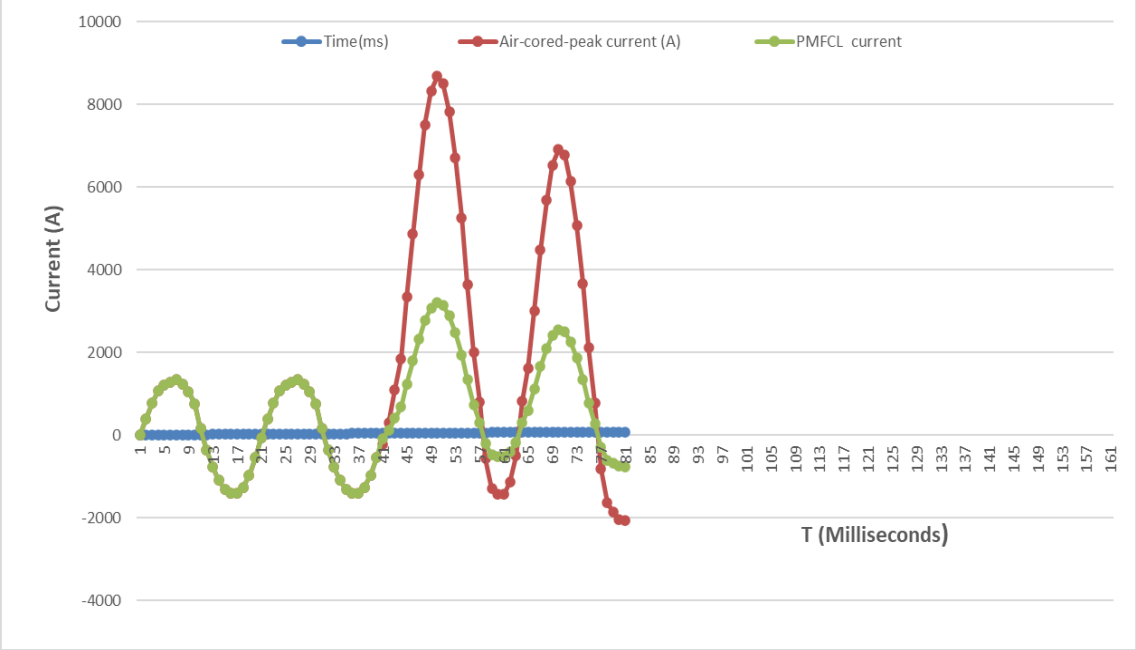

Figure 5 transient current waveform

A nonmagnetic core reactor of similar dimensions to the actual limiter device was simulated to enable a direct comparison of transient performance. The momentary current waveform in Figure 5 shows that the industrial low-voltage PMFCL device limits the peak fault current to approximately 3.22 kA, whereas the air-cored reactor exhibits a peak of 8.7kA. This highlights the substantial reduction in fault current achieved by the ring-shaped PMFCL model. The transient response results also confirm the validity of the inductance–current characteristic curve, as the observed RMS value of the limited peak current aligns closely with predictions from the magnetostatic analysis. Overall, the

industrial PMFCL demonstrates a fault current limiting capability of approximately 63% compared to the air-cored configuration.

Table 2, the model results

Technology	Peak fault current (A)	Device fault current reduction
Current limiter device	**3220**	**63%**
Air-cored	**8700**	**---------**

The state-of-the-art device operates on the principle of magnetic saturation and desaturation within a specially designed magnetic core, typically in a circular shaped topology. The device remains passive under normal conditions but activates automatically when a fault occurs by changing its magnetic impedance characteristics. Figure 6 shows the operation of the fault current limiter during a fault event

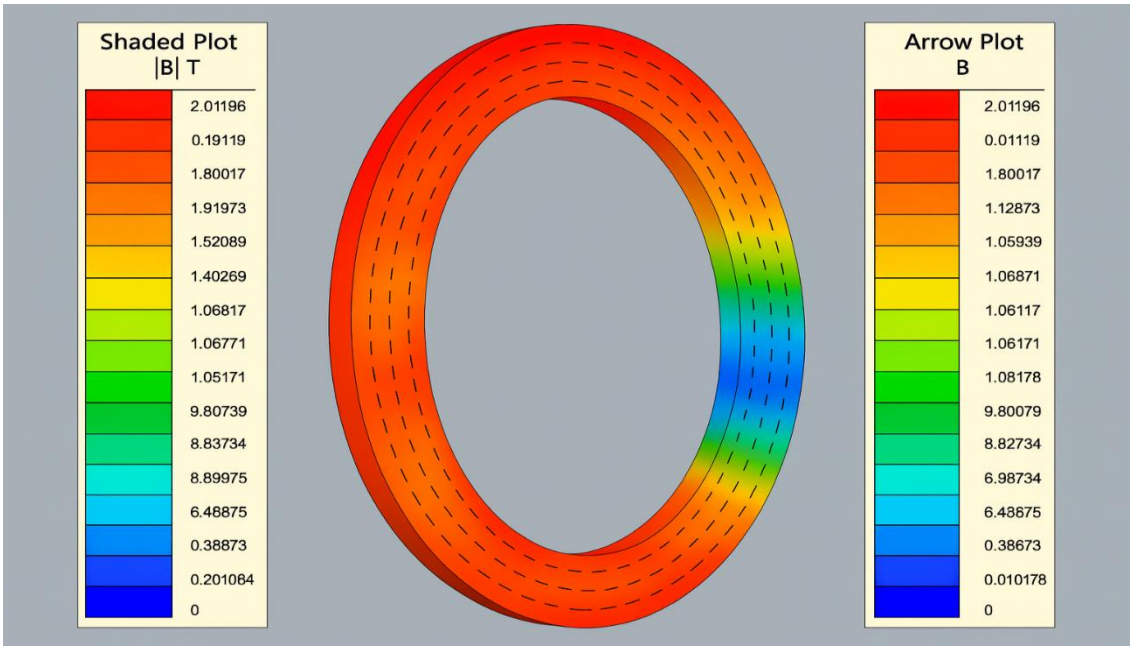

Figure 6 FEM model transient modelling

Once the predicted fault current limit occurred, one segment of the core ring transitions into a state of desaturation. The figure shows the M16 core without AC coils to clearly visualize the core geometry and magnetic flux distribution. The colour scale represents the magnetic flux density B, with red indicating regions of highest magnetic field density of approximately 2.15 T and blue representing the lowest values. This distribution of flux density illustrates the

magnetic behaviour of the core under fault conditions, confirming the device's ability to operate without risk of demagnetization.

Demagnetization analysis of the PMFCL

The demagnetization analysis results for the neodymium magnets were found to lie predominantly in the range of –0.6 to –0.8, corresponding to the blue region of the scale. This indicates that the magnets remain well within the safe operating zone far from the critical demagnetization threshold. This confirms that, even during severe fault currents, the magnets retain their full magnetic integrity. These findings validate PMFCL's ability to operate reliably under fault conditions without the risk of core saturation or permanent magnet demagnetization, ensuring long-term performance and minimal maintenance requirements.

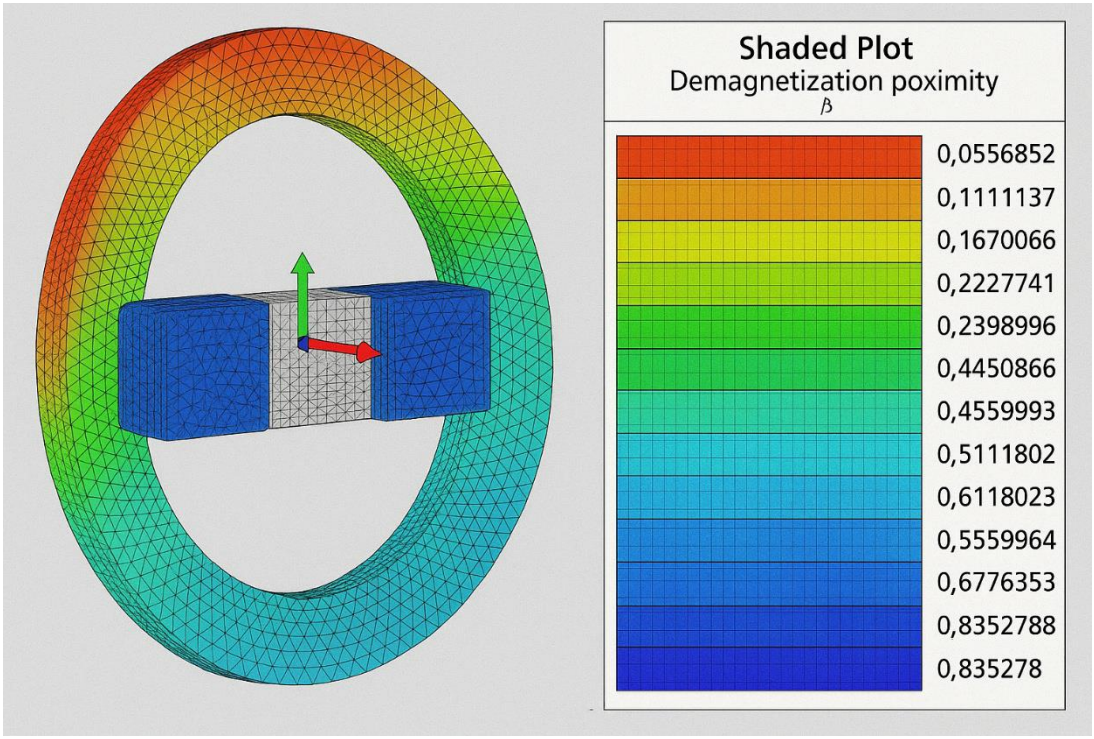

Figure 7 FEM demagnetization analysis

Conclusion and future work

The model presented in this work is an exceptional low voltage industrial power system unit. It is directed to moderate and decrease the extreme short-circuit currents to much more adaptable levels for the existing available switchgear equipment like induction motors, circuit breakers (CBs) and power transformers. Reducing fault current enabling faster, more reliable fault clearing and reducing

voltage severity. Hence, it supports the power system's ability to remain stable after faults. The device functions autonomously and requiring no external power supply for its operation. The permanent magnet provides an acceptable magnetic field to saturate the M16 steel core in the normal working operation.

The PMFCL can be installed to protect the existing 480 Motor Control Centre (MCC) used in oil production plants in Libya. It protects the 480V from excessive fault currents. Additionally, through transformer coupling, the limiter device also helps limit the impact of fault currents on the main feeder 34.5 kV, thereby enhancing protection system across the distribution network. However, the current limiter can also be applied to protect future standby solar power systems, which may be utilised to support the power grid and supply electricity during black start operation of gas turbine units in oil fields.

The effective time modelling of inductance against current graph was obtained using the FEM nonlinear time-harmonic solver developed to predict the device transient characteristics under abnormal conditions. The FEM based flux linkage method is used to create the inductance-current graph. The highest current analysed using FEM nonlinear time-harmonic solver corresponded closely with the maximum surge current attained by simulation tool time step solver. The results are obtained in much less simulation time compared with the extended transient simulation. The inductance current graph shows the highest effective current of 2300A. This value is verified with the extended transient time step solver. The transient simulation in figure 6 shows the maximum fault current of 3220A peak. Thus, the nonlinear time-harmonic solver is the viable time efficient tool used to estimate the maximum transient current at the fault occurrence. The designed unit exhibited exceptionally low insertion impedance during regular operation and a magnificent fault impedance to deliberately enhance the fault current restriction capability at the fault occurrence. The current-limiting reactor of equal length to the proposed unit restricted the fault current to 8700A. In comparison, the candidate unit reduced the fault current to 3220 A, achieving a reduction of nearly 63%. Unlike the traditional current-limiting reactor, which remains permanently connected to the system and causes continuous voltage drop and power losses, the emerging unit offers a more efficient and responsive solution.

An important consideration that needs to be looked at is the impact of existing current transformers (CTs) on the operation of protective relays in the presence of the fault current limiter. Substituting the existing current transformers with specially designed CTs is necessary to maintain reliable protection performance alongside the fault current limiter. However, this process may reduce system reliability due to extended periods of downtime during replacement. The PMFCLs need to be coordinated with the protective relays to confirm the right operation for the switchgear equipment and to evade any unwanted system

outages. In the present power network, the PMFCL should substitute the traditional current limiting reactor to improve the power grid working condition. The new unit provides a slump in the fault current and has a great benefit on the power system network as the motor control centre (MCC) switchgear equipment will work below the rated capacity. Furthermore, the fault current can easily be controlled without spreading to the main feeder and causes more power outages and oil production downtime.

Another key factor to consider when installing the PMFCL device in the power grid is the potential impact of lightning-induced overvoltage on its performance. To address this, the device should undergo high impulse voltage testing in the laboratory to verify its ability to withstand insulation breakdown at elevated voltages before deployment in the power grid.

The simulation results of the designed device showed no demagnetization issues, confirming that the PMFCL can withstand severe fault currents. The dry type ring shaped PMFCL achieves a limiting capability of almost 63%. and successfully restricts the fault current within the first peak cycle.

The future work will involve carrying out a cost-benefit analysis to assess the manufacturing and installation costs relative to the potential long-term economic advantages, such as increased equipment lifespan and reduced maintenance costs. Moreover, several limitations require further consideration, including the scalability of the design and the challenges involved in integrating the technology into existing power system infrastructure. Addressing these issues through further research will be crucial for facilitating extensive adoption and enhancing the overall effectiveness of the device in the existing power system network.

References

1. LEUNG, E. M., et al. (1997). High temperature superconducting fault current limiter development. Applied superconductivity, IEEE transactions on, 7 (2), 985-988.
2. Safaeia, M. Zolfaghariab, M. Gilvanejada, and G. B. Gharehpetianb, “A survey on fault current limiters: Development and technical aspects,” Int. J. Elect. Power Energy Syst., vol. 118, 2020, Art. no. 105729.
3. W. V. S. Azevêdo, et al. (2010). Device to limit Transient Recovery Voltage. 2010 IEEE/PES transmission and distribution conference and exposition: Latin america (T&D-LA), 1-6.
4. Sotelo, G. G., dos Santos, G., Sass, F., França, B. W., Dias, D. H. N., Fortes, M. Z., . . . de Andrade Jr, R. (2022). A review of superconducting fault current limiters compared with other proven technologies. Superconductivity, 3, 100018.

5. Liang Zou, et al. (2009). Study on the feasibility of developing high voltage and large capacity permanent-magnet-biased fault current limiter. Universities Power Engineering Conference (UPEC), 2009 Proceedings of the 44th International, 1-5. 7
6. Farzinfar, M., & Jazaeri, M. (2020). A novel methodology in optimal setting of directional fault current limiter and protection of the MG. *International Journal of Electrical Power & Energy Systems, 116,* 105564. doi:10.1016/j.ijepes.2019.105564
7. J. Linden, Y. Nikulshin, A. Friedman, Y. Yeshurun and S. Wolfus, "Phase-Coupling Effects in Three-Phase Inductive Fault-Current Limiter Based on Permanent Magnets," in *IEEE Transactions on Magnetics*, vol. 56, no. 2, pp. 1-7, Feb. 2020, Art no. 8600107, doi: 10.1109/TMAG.2019.2956147.
8. Rai, S., De, M. (2020). Optimal Placement of Resistive Superconducting Fault Current Limiters in Microgrid. In: Singh, S., Pandey, R., Panigrahi, B., Kothari, D. (eds) Advances in Power and Control Engineering. Lecture Notes in Electrical Engineering, vol 609. Springer, Singapore. https://doi.org/10.1007/978-981-15-0313-9_6
9. SANTRA, T., et al. (2009). Analysis of passive magnetic fault current limiter using wavelet transforms. In: Power Systems, 2009. ICPS '09. Internatio
10. Li, Q., Xu, J., Zou, L., & Lou, J. (2012). Modelling methodology and experimental verification of the permanent-magnet-biased saturation-based fault current limiter. Electric Power Applications, IET, 6(8), 504-512.
11. J. Zhao, Z. Wu, H. Long, H. Sun, X. Wu, C. Chan, & M. Shahidehpour. (2024). Optimal operation control strategies for active distribution networks under multiple states: A systematic review. Journal of Modern Power Systems and Clean Energy, 12(5), 1333–1344. doi:10.35833/MPCE.2023.000372
12. https://electrical-engineering-portal.com/download-center/books-and-guides/power-substations/switchgear-mccs-oil-industry
13. https://www.esi-africa.com/renewable-energy/libya-500mw-solar-project-lined-up/
14. El-Ela, A.A.A.; El-Sehiemy, R.A.; Shaheen, A.M.; Ellien, A.R. Review on Active Distribution Networks with Fault Current Limiters and Renewable Energy Resources. Energies 2022, 15, 7648. https://doi.org/10.3390/en15207648
15. Magnet user manual by Infolytica, www.infolytica.com.
16. Zubkov, Y. V., & Vladimirov, D. A. (2020). Selection of permanent magnet material for starter excitation. Paper presented at the 2020 International Multi-Conference on Industrial Engineering and Modern Technologies (FarEastCon), 1–6.

17. Grimmond, W., Moses, A. J., & Ling, P. C. (1989). Geometrical factors affecting magnetic properties of wound toroidal cores. IEEE Transactions on Magnetics, 25(3), 2686–2693